Reference: *Biol. Bull.* **211:** 183–192. (October 2006)

Study of Larval and Adult Skeletogenic Cells in Developing Sea Urchin Larvae

MAMIKO YAJIMA AND MASATO KIYOMOTO*

Tateyama Marine Laboratory, Marine and Coastal Research Center, Ochanomizu University, 11 Koyatsu, Tateyama, Chiba 294-0301, Japan

Abstract. The larval skeleton of sea urchin embryos is formed by primary mesenchyme cells (PMCs). Thereafter, the larvae start feeding and additional arms develop. An adult rudiment that contains spines, tube feet, tests, and other parts of the adult body is formed in the eight-armed larva. The cellular mechanism of the later skeletogenesis and the lineage of the adult skeletogenic cells are not known. In this study, the morphogenesis of larval and adult skeletons during larval development of the sea urchin *Hemicentrotus pulcherrimus* was investigated by immunostaining cells with PMC-specific monoclonal antibodies, which are useful markers of skeletogenic cells. All spicules and the associated cells in the later larvae were stained with the antibodies. We could observe the initiation of skeletal morphogenesis at each developmental stage and visualize the cellular basis of skeleton formation in whole-mount embryos that possessed an intact morphology. There were some similarities between PMCs and the later skeletogenic cells. Both had a rounded shape with some filopodia, and the antigen expression started just before overt spicule formation. In the later-stage embryos, cells with filopodia and faint antigen expression were observed migrating in the blastocoel or aggregating in the presumptive location of new skeletogenesis.

Introduction

The adult rudiment, which is an adult organ formed in a part of the larval body in echinoderms, has been attracting interest from embryologists and cell biologists for a long time (Wilt, 2002). In sea urchins, the adult rudiment is formed in the left part of the larval body at the eight-armed pluteus stage, and it contains most of the adult tissues, such as tube feet, spines, and tests. At metamorphosis, larval structures are degraded, and the adult rudiment emerges from inside the larval body. However, the details of rudiment formation, such as cell lineages, cell differentiation, or gene regulatory systems during adult organogenesis, are still unknown.

As the part of development that leads the animal to its last developmental stage—the adult—metamorphosis is as important a subject of study as embryogenesis. Indirect development, including metamorphosis, is thought of as an evolutionally ancestral developmental style because it is common in marine animals and is seen in diverse animal phyla. While development from embryo to larva is slow and continuous, metamorphosis from larva to adult is quick and discontinuous. This drastic morphological change is driven by the events at the cellular level under the regulation of cell-to-cell signaling and gene expression. Studies on a cellular basis are essential for understanding the complicated phenomenon of metamorphosis. The sea urchin is ideal for a detailed study of the mechanisms of late development and metamorphosis because it has been a popular experimental animal for decades and the literature on its development is extensive.

Skeletogenesis is an essential part of constructing the framework for an animal's body, and it defines the body plan in various groups such as vertebrates, echinoderms, and molluscs. Echinoderms possess elaborate calcareous endoskeletons. In sea urchin embryos, because of the simplicity of the formation of their spicules and the transparency of their tissues, morphogenesis and differentiation of the spicules have always attracted researchers' attention and have been studied using both classical and molecular ap-

Received 2 February 2006; accepted 24 May 2006.

* To whom correspondence should be addressed. E-mail: kiyomoto@cc.ocha.ac.jp

Abbreviations: PBSC, phosphate-buffered saline saturated with calcite; PMC, primary mesenchyme cell; SMC, secondary mesenchyme cell; SW, seawater.

proaches. Consequently, there is considerable information about proteins and genes in relation to the formation of embryonic spicules (Anstrom and Raff, 1987; Killian and Wilt, 1996; Wilt, 1999, 2002; Davidson *et al.,* 2002). In contrast, skeletogenesis in the later larvae and in the adult has rarely been studied.

Spicules of the sea urchin embryo are synthesized by primary mesenchyme cells (PMCs), which are descendants of the micromeres of the 16-cell-stage embryo (Gustafson and Wolpert, 1967; Okazaki, 1975; Ettensohn *et al.,* 1997). The PMCs ingress at the blastula stage and are arranged in a characteristic ring pattern (PMC-ring), then form a triradiate skeletal rudiment in each of the two cell clusters on the ventrolateral aspects of the PMC-ring (Ettensohn *et al.,* 2000). These skeletal rudiments subsequently elongate and branch out in a characteristic form, giving rise to the skeletal rods of the prefeeding four-armed pluteus larva. A few descriptions related to the skeletal morphogenesis of sea urchin have been reported (Hyman, 1955; Dubois and Chen, 1989), especially that of Gordon (1926), who carefully observed skeletogenesis in the adult rudiment by using classical methods (maceration and clearing larvae with NaOH and glycerin).

Several PMC-specific proteins that participate in the synthesis of the skeleton have been obtained, and in the present study, we used PMC-specific antibodies that recognize the carbohydrate epitopes of msp130, a 130-kDa membrane glycoprotein specific to PMCs (Shimizu-Nishikawa *et al.,* 1990; Kominami and Takaichi, 1998). Expression of msp130 has been reported in both embryo and adult tissues (Anstrom and Raff, 1987; Parks and Raff, 1988; Drager *et al.,* 1989); spicule matrix proteins such as SM30 and SM50 were also observed (see review by Wilt, 2002). Although the expression of some genes is common between embryonic and adult skeletogenesis, the cell lineage of adult skeletogenic cells is not known. We investigated skeletogenesis in the late larvae and in the adult rudiment on a cellular basis by immunostaining the skeletogenic cells in whole-mount intact larva, paying particular attention to tissues associated with spicules and examining the process of skeletogenesis in the later development of sea urchin larvae. As illustrated in Figure 1, many kinds of spicules are formed in the late larval stage. Some of them are formed from the branches of larval rods, such as three of five genital plates and two of five terminal plates (Gordon, 1926). Other skeletal elements are newly produced in the larval body or in the adult rudiment. In this study we focused on these newly formed spicules to examine how skeletogenic cells appear.

Materials and Methods

Animals and embryos

Adult specimens of *Hemicentrotus pulcherrimus* Agassiz (1863) were collected from the seashore of Boso Peninsula, Japan. Gametes and sperm were obtained by injection of 10 mmol l^{-1} acetylcholine chloride into the coelomic cavity. Eggs were washed several times with filtered natural seawater (SW). Dry sperm were kept at 4 °C until use. Eggs were fertilized and washed several times in SW and then cultured at 18 °C.

Larval culture

Larvae of *H. pulcherrimus* were transferred to a 2-l beaker after hatching (13 h after fertilization) and reared according to the method of Noguchi (1978), with slight modifications. Previously, filtered SW was sterilized by heating it at 80 °C for 30 min. At the onset of feeding (2–3 days after fertilization), approximately 20,000 pluteus larvae were cultured at 19 °C in 2 l of sterilized SW that was gently stirred with a paddle connected to a 30-rpm motor. Two-thirds of the culture water was renewed twice weekly. From the third day after fertilization, two types of diatoms, *Chaetoceros gracilis* Schutt 1895 and *C. calcitrans* (Paulsen) Takano 1968, were supplied twice weekly to the

Figure 1. Schematic representation of the larval development of *Hemicentrotus pulcherrimus.* The outline of larval morphology at each stage from the four-armed pluteus to the late eight-armed pluteus is shown. *Abbreviations:* al, anterolateral rod; amn, amniotic invagination; da, dorsal arch; d-sp, dorsal spine; d-tf, disk of primary tube foot; gen, genital plate; hyd, hydrocoel; int, interambulacral plate; pd, posterodorsal rod; po, post-oral rod; pr, pre-oral rod; ter, terminal plate; tf, primary tube foot; v-sp, ventral spines. (A) Late four-armed pluteus stage, dorsal view. (B) Early six-armed pluteus stage, dorsal view. The rudiment of the posterodorsal rod (pd) and dorsal arch (da) are formed. (C) Late six-armed pluteus stage, dorsal view. The posterodorsal rods and dorsal arch are well elongated and form characteristic shapes. Infolding of amniotic invagination (amn) and the development of hydrocoel (hyd) begins from adult rudiment. (D) Early eight-armed pluteus stage, lateral view from left side. The adult rudiment is developed and the rudiments of the primary tube foot (tf) are formed. (E) Middle eight-armed pluteus stage, dorsal view. The rudiments of the dorsal spines (d-sp), ventral spines (v-sp), and the disk of the primary tube foot (d-tf) are formed in the adult rudiment. Three of five genital plates (gen) and two of five terminal plates (ter) are formed from branches of larval rods. (F) Late eight-armed pluteus stage, dorsal view. Larvae have a full-grown rudiment and are competent for metamorphosis. The dorsal spines are located adjacent to the terminal plates (ter), and the ventral spines are on the interambulacral plates (int). Dorsal spines are also on the genital plates outside of the adult rudiment. (G) Late eight-armed pluteus stage, lateral view from left side. The sacks of ectodermal cell sheet covering spines and tube feet are omitted in E, F, and G.

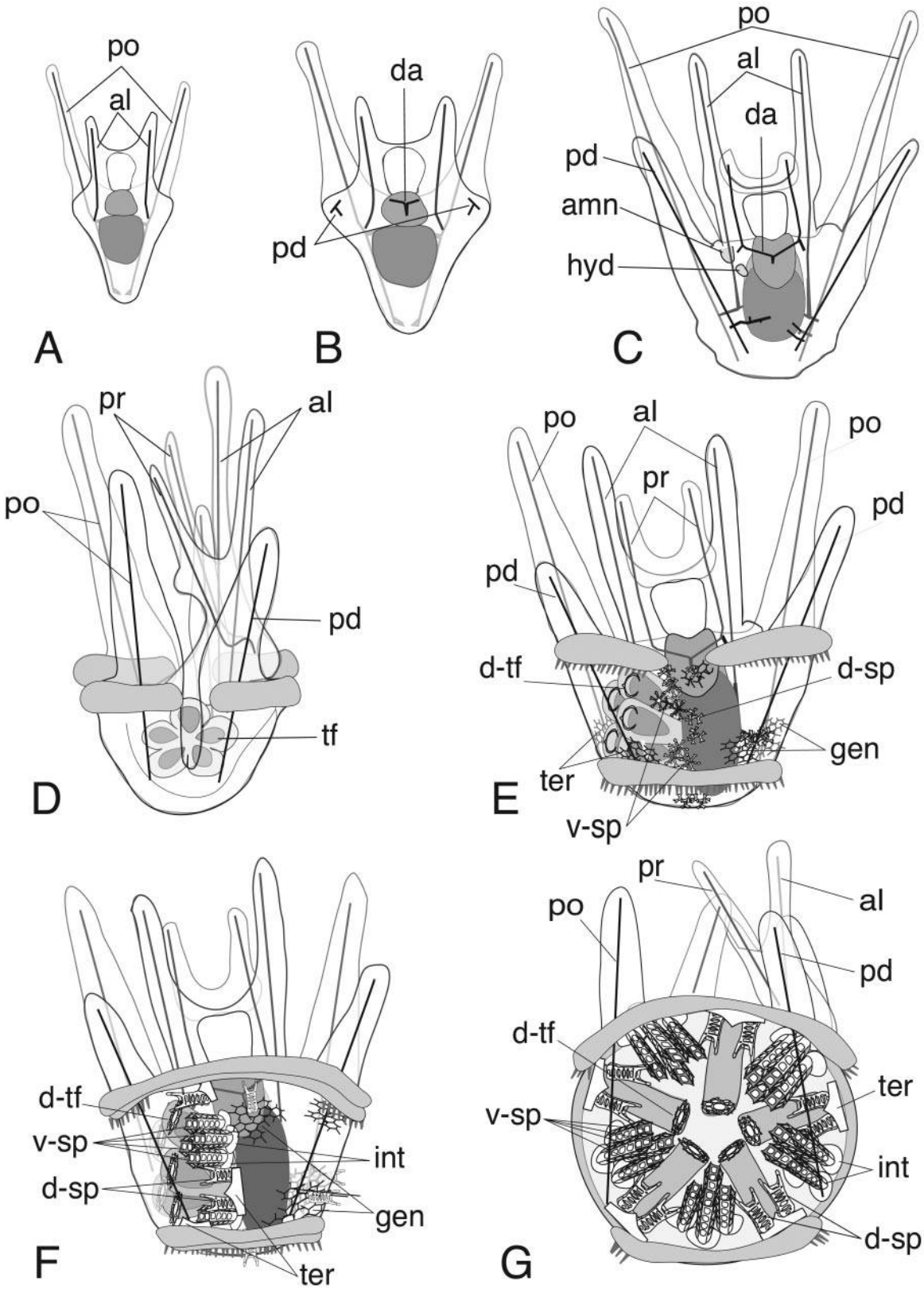

cultures, each beaker receiving 3–4 ml of each diatom at a concentration of 3–5 $\times$ 10^6 ml. The larval density was initially 10 larvae/ml but was diluted to 1 larva/ml at the stage of the eight-armed pluteus. Larvae reached the early six-armed stage after 10–14 days and the middle eight-armed stage after 3–4 weeks.

Calcein labeling

To distinguish skeletogenic cells from spicules, the larvae whose spicules were labeled with calcein (Guss and Ettensohn, 1997) were used for immunostaining. Calcein (Dojindo, Kumamoto, Japan) was dissolved at 2.5 mg/ml in SW, pH 8.3, and stored at 4 °C. At 24 h post-fertilization, embryos were cultured in 50 μg/ml calcein SW; the rest of the culturing method was the same as that used for normal larvae.

Culture of diatoms

Chaetoceros gracilis was cultured in a medium that contained 180 ml of filtered SW; 120 ml of distilled water; 6 ml of stock solution A containing 10 g $NaNO_3$, 500 mg sodium β-glycerophosphate, 500 mg sodium iron EDTA, 3 g Clewat-32 (Teikoku Co., Ltd., Tokyo, Japan), 10 mg vitamin B_{12}, and 5 g HEPES (pH 7.0) in 1000 ml of distilled water; and 0.75 ml of stock solution B containing 14–20 g $NaSiO_3$ per liter. *C. calcitrans* was cultured in 300 ml SW that was supplemented with 23 mg $NaSiO_3$ and 0.3 ml KW21 (Daiichi Seimo Co. Ltd., Arao, Japan). Both culture media were sterilized by heating at 70–80 °C for 30 min, and then cooled to 18–20 °C before use. Diatoms were cultured and aerated under a 60-watt light bulb at 18–20 °C.

Differential interference contrast microscopy and polarizing microscopy

The skeletogenesis of the posterodorsal rod, dorsal arch, disk of tube foot, and spines were observed with differential interference contrast (DIC) microscopy and polarizing microscopy (OPTIPHOT-POL, Nikon, Tokyo, Japan).

Immunostaining and microscopy

Two PMC-specific monoclonal antibodies, P4 (Shimizu-Nishikawa *et al.,* 1990) and IG9 (Kominami and Takaichi, 1998), were used to identify skeletogenic cells by indirect immunofluorescence staining. These monoclonal antibodies had been shown to recognize the carbohydrate epitopes of msp130, a 130-kDa membrane glycoprotein specific to PMCs (Shimizu and Matsuda, 1988; Kominami and Takaichi, 1998; Shimizu-Nishikawa *et al.,* 1990).

For whole-mount immunostaining, the larvae of each stage from early six- to late eight-armed plutei were fixed with cold methanol (−30 °C) in a 24-well plate for 1 h. Fixed larvae were rinsed twice at 30-min intervals in phosphate-buffered saline saturated with calcite (bleached adult tests). This saturated buffer (PBSC) was used throughout the staining procedure to minimize demineralization of spicules and to facilitate the identification of spicule regions after staining. Washed specimens were transferred to a 96-well plate. Specimens were immunostained individually in each well with monoclonal antibody, either P4 (at a dilution of 1:100–1:1000) or IG9 (undiluted), for 5 h at room temperature. After the rinse with PBSC under the same conditions, specimens were then reacted with Alexa Fluoro 488 (or Alexa Fluoro 594 for calcein-labeled larvae) goat anti-mouse immunoglobulin G (IgG) antibody (Molecular Probes, Carlsbad, California, USA) for 5 h at room temperature in the same manner as for P4 or IG9. After the rinse with PBSC under the same conditions again, larvae were mounted on a glass slide, and a drop of mounting medium (10% 1,4-diazabicyclo [2.2.2] octane and 50% glycerin in PBSC) was added before a coverslip was placed over it. Stained larvae were observed using confocal laser scanning microscopy (Leica, TCS/NT, Tokyo, Japan).

Results

Development of posterodorsal rod and dorsal arch

The rudiments of posterodorsal rods (see Fig. 1B; pd) and dorsal arch (Fig. 1B; da) are formed at the early six-armed stage (Fig. 2A). In the formation of posterodorsal rods, first a granule-like skeletal rudiment appeared on each lateral side of the larval body (stage 1; Fig. 2B: b, arrow). These two skeletal rudiments grew and formed triradiate spicules (stage 2; Fig. 2C: c, arrow), then elongated and eventually became the posterodorsal arms in the late six-armed pluteus (stage 3; Fig. 2D). The skeletal rudiment of the dorsal arch appeared slightly after those of the posterodorsal rods. It started from a small skeletal rudiment (stage 1; Fig. 2E: e, arrow) and soon became triradiate; two branches elongated rapidly (stage 2; Fig. 2F: arrow) and eventually developed into pre-oral arms in an eight-armed pluteus (stage 3; Fig. 2G: arrow).

Immunostaining revealed several skeletogenic cells in a cluster at the site where each skeletal rudiment of the posterodorsal rod (Fig. 3A: arrows) and dorsal arch (Fig. 3A: arrowhead) would be formed, but the cluster appeared just prior to the appearance of skeletal rudiments. A granule-like or tiny triradiate skeletal rudiment was then formed in each cell cluster (stage 1; Fig. 3B, C: arrows and arrowhead). One branch of the triradiate rudiment of the posterodorsal rods and two branches of the rudiment of the dorsal arch then extended (stage 2; Fig. 3D). An extended branch gave rise to the rod that supports the posterodorsal arms in a six-armed pluteus. The dorsal arch elongated more slowly but eventually became the pre-oral rods in an eight-armed pluteus (stage 3). The skeletogenic cells moved along the spicule rods as they elongated.

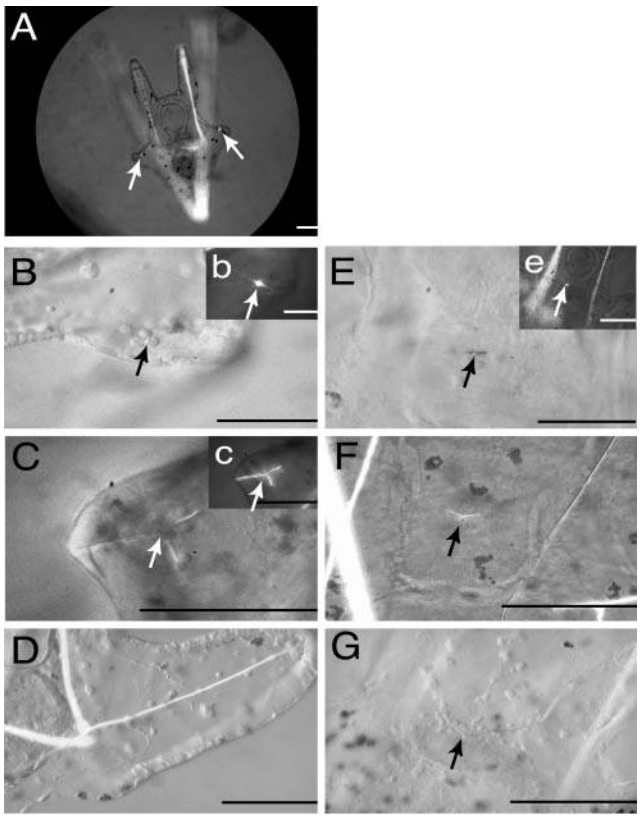

Figure 2. Development of the posterodorsal rod and dorsal arch of a six-armed pluteus larva viewed with differential interference contrast microscopy (B–G) and with polarizing microscopy (A, b, c, e). (A) The early six-armed stage. A tiny crystal that is observed on each lateral side of larval body (arrows) is a rudiment of the posterodorsal rod. A rudiment of the dorsal arch has not been formed. (B and b) Stage 1: a magnified view of the posterodorsal arms. A tiny skeletal rudiment (arrows) is surrounded by three cells. (C and c) Stage 2: a triradiate rudiment of the posterodorsal rod (arrows) starts elongating, and the associated cells also migrate together along the skeletal rod. (D) Stage 3: a posterodorsal rod (arrow) has been elongated enough to support the larval new arm. (E and e) Stage 1: a magnified view of the rudiment of a dorsal arch (arrows). A skeletal rudiment is formed at the early six-armed stage just after the formation of the rudiment of the posterodorsal rod. (F) Stage 2: a triradiate spicule of the dorsal arch (arrow) is observed. Many cells are accumulated around the skeletal rudiment. (G) Stage 3: two branches of the triradiate spicule of the dorsal arch (arrow) elongate rapidly and form a typical shape. These two branches give rise to pre-oral rods in the eight-armed stage. Bar = 50 μm.

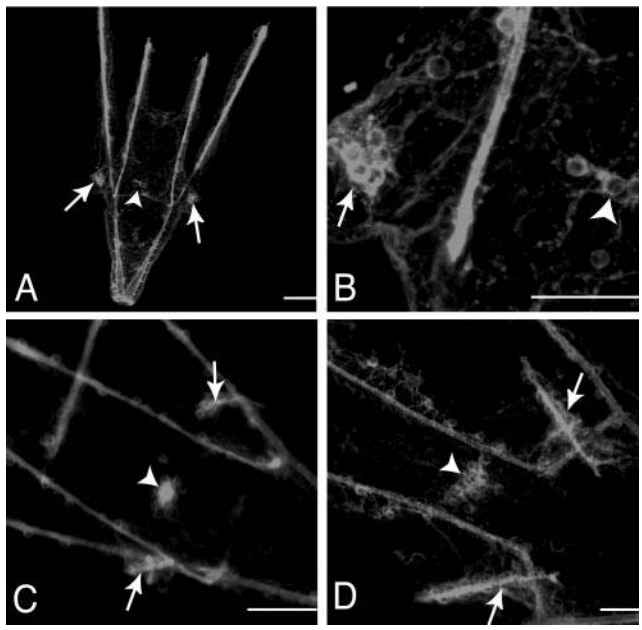

Figure 3. Micrographs of a six-armed pluteus, immunostained with a primary mesenchyme cell (PMC)-specific monoclonal antibody, P4. All images were obtained by using confocal laser-scanning microscopy. (A and B) Stage 1: early six-armed pluteus (A, whole embryo; B, magnified view of the posterodorsal rod and dorsal arch). Stained cells suddenly appear in a cluster at the sites where the skeletal rudiments of the posterodorsal rod (arrows) and the dorsal arch (arrowheads) will be formed. (C and D) Stage 2: Early (C) to middle (D) stage of the six-armed pluteus. Skeletal rudiments of the posterodorsal rods start to elongate in C (arrows), and were long enough to support the posterodorsal arms in D (arrows). A skeletal rudiment of the dorsal arch is formed in C (arrowhead) and triradiately elongated in D (arrowhead). Bar = 50 μm.

Development of the disk of the primary tube foot

The disk of the primary tube foot (Fig. 1E–G: d-tf) is a skeletal element formed at the tip of the primary tube foot, just prior to the spine formation at the middle of the eight-armed pluteus stage. It started from a tiny stick-shaped spicule (stage 1; Fig. 4A: a, arrow), but soon rapidly elongated and formed a simple skeletal ring (stage 2; Fig. 4B, C). Once the circle of the ring was completely formed, several skeletal branches appeared from the simple ring. These elongated branches soon divided dichotomously and met at the end; then, from this mesh-like ring, the disk of the primary tube foot was formed (stage 3; Fig. 4D). The process of disk formation is shown in Figure 4E.

During the immunostaining process, the skeletogenic cells were observed first at the tip of the tube foot, where they were arranged in a ring, prior to formation of the skeletal disk (stage 1; Fig. 5A). In one specimen, a couple of skeletogenic cells were observed in a tube foot (Fig. 5B). The skeletogenic cells maintained the ring-shaped arrangement and formed a simple skeletal ring (stage 2; Fig. 5C). Thereafter, the arrangement of cells became disordered, making a mesh-like skeletal ring that was a unique formation of the disk (stage 3; Fig. 5D).

Development of the dorsal and ventral spines

There are two types of spines in the sea urchin, a dorsal spine and a ventral spine, both of which started to form at the middle eight-armed stage (Fig. 1E–G: d-sp, v-sp). The formation of the ventral spine began in a granular skeletal rudiment near the base, inside the adult rudiment (stage 1: Fig. 6A: a), and this granular rudiment grew into a hexa-

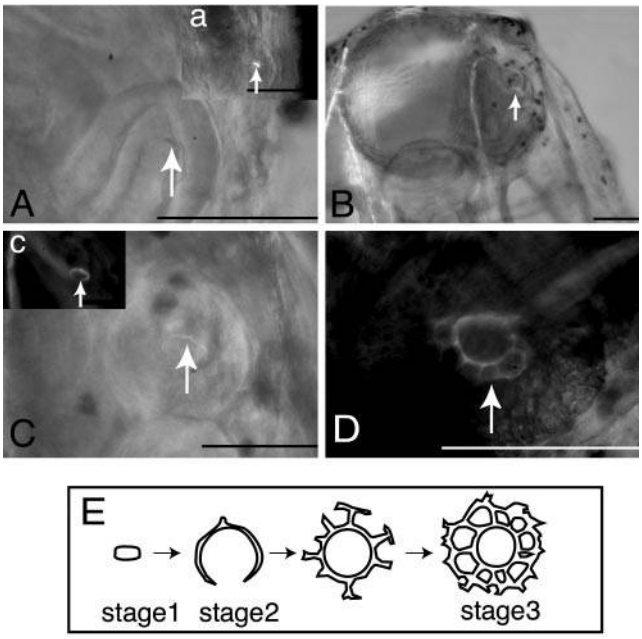

Figure 4. Development of the disk of the primary tube foot viewed with differential interference contrast microscopy (A–C) and polarizing microscopy (a, c, D). (E) Illustration of the disk formation. (A and a) Stage 1: a tiny spicule is formed on the inner wall side of the primary tube foot (arrows) at the middle eight-armed stage. (B, C and c) Stage 2: a simple skeletal ring is formed on the tip of the tube foot (arrows). (D) Stage 3: a complete ring is apparent. Several skeletal branches appear from the ring, and some of them have already branched off and met at the other end. A mesh-like ring eventually develops at the late eight-armed stage. Bar = 50 μm.

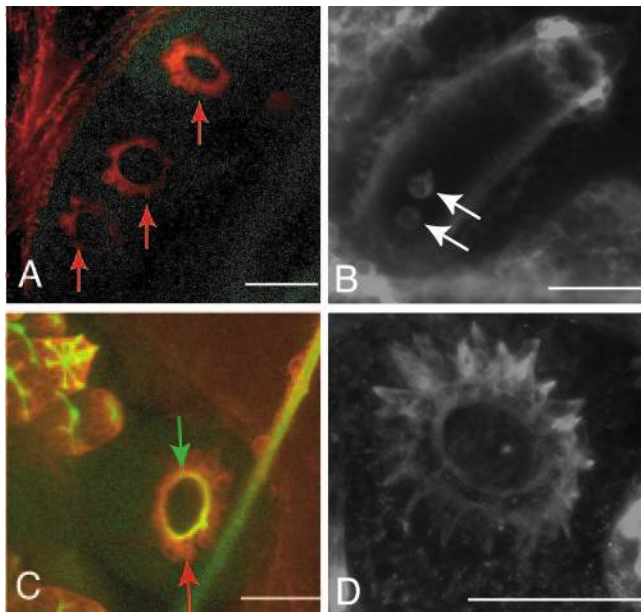

Figure 5. Immunostaining of the disk of the primary tube foot with a primary mesenchyme cell (PMC)-specific monoclonal antibody, P4. For double staining, P4 is shown in red and calcein in green. All images were observed by using confocal laser-scanning microscopy. (A and B) Stage 1: tube feet in the adult rudiment of middle stage of the eight-armed pluteus. Cells start lining up at the tip of the tube foot (arrows in A). A magnified view shows a couple of cells in a tube foot (arrows in B). (C) Stage 2: the lined-up cells (red arrow) start forming a simple skeletal ring (green arrow), which is the disk rudiment. (D) Stage 3: a line of cells at the tip of tube foot becomes disordered, and the cells make a mesh-like skeletal ring unique to the disk of the primary tube foot. Bar = 50 μm.

radiate spicule (Fig. 6B: mb and b). The hexaradiate spicule then elongated perpendicularly and became a three-dimensional crystal structure (Fig. 6C, c). A ventral spine rudiment and a rudiment of the interambulacral plate (Fig. 6C, arrow) were formed together in a sack made of sheets of ectodermal cells. This cell sheet was derived from amniotic invagination (Fig. 1C: amn). The ventral spine rudiment lengthened into a spine with a ladderlike rod with six branches (Fig. 6D: d; arrowheads). A branch of the interambulacral plate was situated at the base of the developing spine in Figure 6D (arrows).

The dorsal spine began from a granular skeletal rudiment and soon became triradiate (Fig. 6E: e and me, arrow), appearing both inside and outside the adult rudiment (Fig. 6E, F: arrows). Each branch of the triradiate spicule elongated and dichotomized at the tip, and then a vertical process arose from the halfway point of each branch (Fig. 6F: f). Two of the three vertical processes grew straight up and were connected with a horizontal branch. Each vertical process continued to grow to form a main branch of the dorsal spine, while the third one branched dichotomously and elongated into two main branches of the dorsal spine. Finally, a spine with four tips was formed (Fig. 6G: mg and g). The spines were elongated and formed ladderlike shapes with four branches (Fig. 6H: h). A meshwork of a terminal plate, similar to that of an interambulacral plate in the case of a ventral spine, was built up under the base of the dorsal spine. Two dorsal spines were located at a terminal plate (Fig. 6H: arrow heads).

During immunostaining, several skeletogenic cell aggregates forming a spherical smooth surface were first observed prior to spicule formation at the early eight-armed stage (Fig. 7A, B). The rudiments of spines developed at the spherical side in these cell aggregates (Fig. 7C and D: yellow arrows). At the basal side of each cell aggregate, the rudiment of the interambulacral plate was formed (Fig. 7D: white arrows). When the rod of a spine began to appear, the outlines of each stained cell on the spine became indistinct (Fig. 7E: arrows), while those at the bottom remained obvious (Fig. 7E: arrowheads). A unique ladderlike formation of the spine became recognizable after their elongation, as shown in Fig. 7F (arrows indicate the ventral spines and arrowheads indicate the dorsal spines).

Appearance of "later skeletogenic cells"

In larval spicules and in the adult rudiment, the initial appearance of P4 antigens in the "late skeletogenic cells"

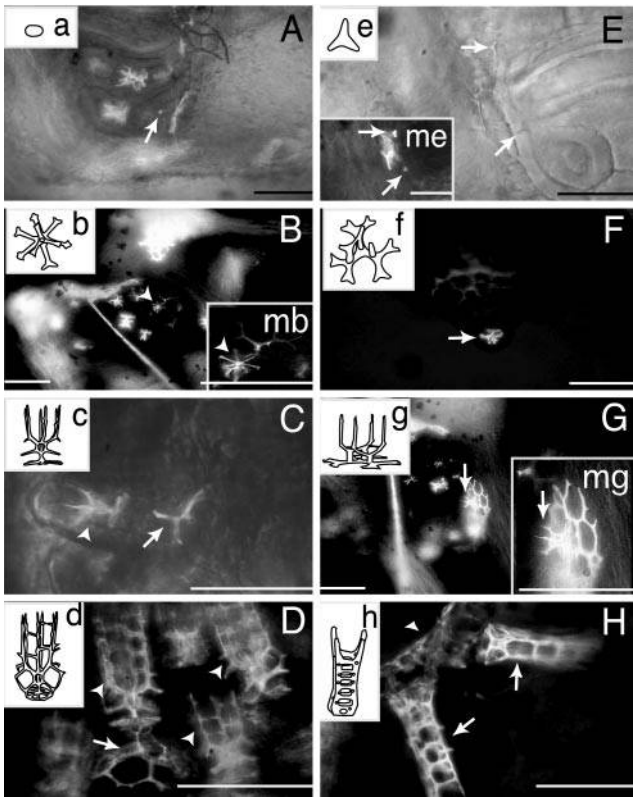

Figure 6. Development of the ventral spine (A–D) and the dorsal spine (E–H) of the middle eight-armed pluteus larvae, viewed using differential interference contrast microscopy (E) and polarizing microscopy (A–D, F–H, mb, me, and mg) and drawn in illustrations (a–h). Bar = 50 μm. *Ventral spine.* (A and a) Stage 1: a granule-like skeletal rudiment appears near the inside base of the adult rudiment (arrow). (B, mb, and b) Stage 2: the granule-like skeletal rudiment has grown into a hexaradiate spicule (arrowhead in B and mb; mb is a magnified view of the rudiment). (C and c) Stage 3: the hexaradiate spicule is elongated perpendicularly and becomes a 3-D crystal structure (arrowhead). Another spicule located in the basal side of ectodermal cell sack is a rudiment of the interambulacral plate (arrow). (D and d) Stage 4: the skeletal rod lengthens and becomes a ladder-like spine with six branches (arrowheads). A branch of an interambulacral plate (arrows) is situated immediately below the developing spine. *Dorsal spine.* (E, e, and me) Stage 1: a triradiate skeletal rudiment (arrows) is observed right on the base of adult rudiment. (F and f) Stage 2: each branch of the triradiate lengthens, and a vertical process arises from the middle of each of the three branches (arrow). (G, mg, and g) Stage 3: two of three vertical processes grow straight up, and each forms a prong. The third process also arises perpendicularly but soon branches dichotomously and forms two prongs, and a spine with four branches is formed (arrows in G and mg; mg is a magnification of dorsal spine). (H and h) Stage 4: the spine is elongated and forms a ladder-like shape with four branches (arrows). A meshwork of a terminal plate is built up under the base of a spine. Two dorsal spines are apparent on one terminal plate (arrowhead).

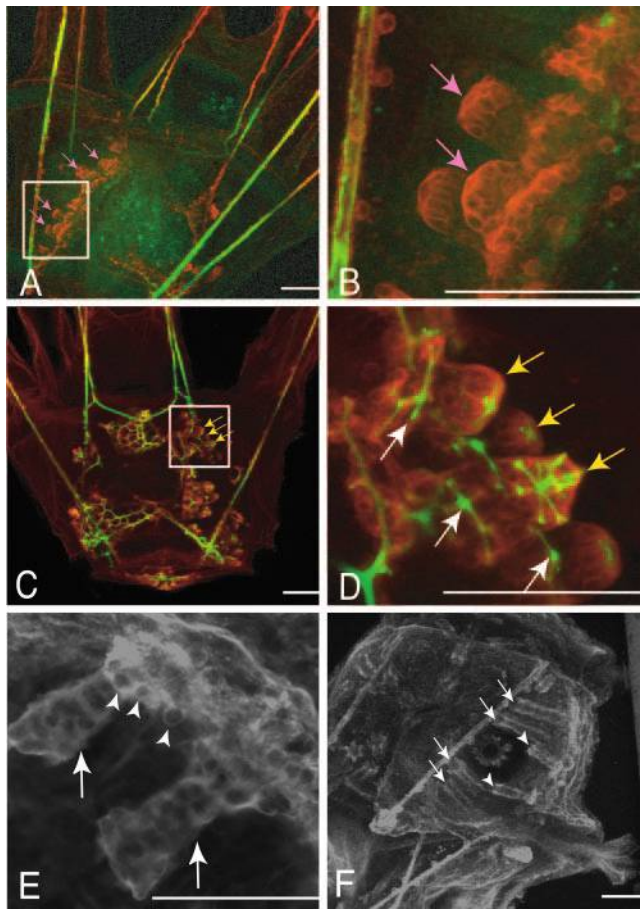

Figure 7. Indirect immunofluorescence with a primary mesenchyme cell (PMC)-specific monoclonal antibody, P4. For double staining, indirect immunofluorescence with P4 is indicated in red and direct fluorescence with calcein is indicated in green. All images were obtained by using confocal laser-scanning microscopy. Bar = 50 μm. (A and B) Stages 1 and 2: the middle eight-armed stage of pluteus larvae. Several skeletogenic cell aggregates appear at the bottom of the adult rudiment (arrows). In a magnified view (B), typical skeletal rudiments are not recognizable. Skeletogenic cell aggregates were completely stained (arrows). (C and D) Stage 3: a rod of ventral spine (yellow arrows) and a rudiment of interambulacral plate (white arrows) begin to appear from the cellular sack. (E and F) Stage 4: the late stage of an eight-armed pluteus. Outlines of cells at the bottom are obvious (E, arrowheads), while those on the skeletal rod become inconspicuous (E, arrows). The spine is well elongated and a unique ladder-like form is now recognizable (F). Spines with four branches are peculiar to the dorsal spine (F, arrowheads), and one with six branches is typical of the ventral spine (F, arrows).

resembled that in PMCs. The P4 antigen first appeared as intracellular spots in the presumptive skeletogenic cells. It was then detected weakly in the cytoplasm and on the surface of the skeletogenic cells (Fig. 8B). When spicule formation began, the P4 antigen covered the entire surface of the cells, and as a result, the staining intensity of the skeletogenic cells increased (Fig. 8A: arrow). This pattern of P4 antigen expression is similar to that of PMCs (see fig. 4 in Shimizu and Matsuda, 1998). The initial formation of the dorsal arch was observed, as shown in Figure 8A and B. P4 reacted strongly with cells related to the posterodorsal rod, which was formed slightly before the dorsal arch; P4 reacted weakly with cells related to the dorsal arch, which was about to be formed. The cells stained weakly with P4 are seen in the blastocoel of the six-armed pluteus (Fig. 8C:

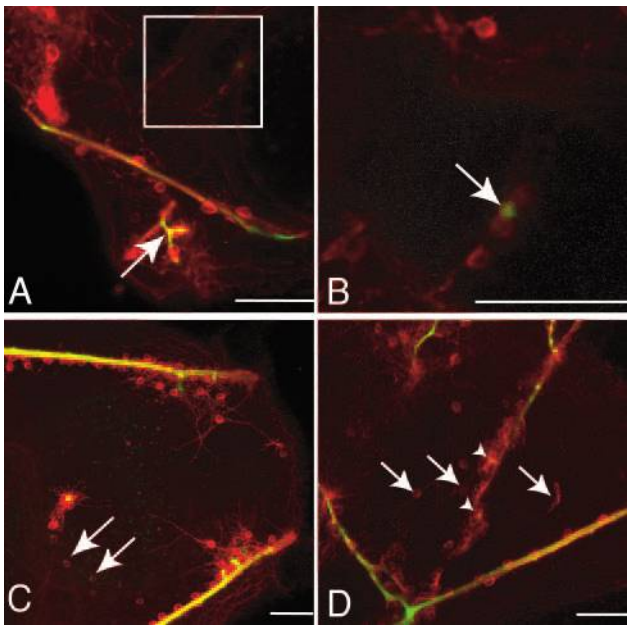

Figure 8. Indirect immunofluorescence with primary mesenchyme cell (PMC)-specific monoclonal antibody, P4 (red) and direct fluorescence with calcein (green) obtained by using confocal microscopy. In these figures, sensitivity to immunofluorescence was highly increased. (A–B) Early six-armed pluteus. The P4 reacted strongly with cells related to the posterodorsal rod (arrow), while it reacted weakly with ones related to the dorsal arch (square). B is the magnified view in the square of A. The rudiment of dorsal arch is formed (arrow). (C) Late six-armed pluteus. The cells stained weakly with P4 (arrows) appear to be stretching their filopodia and migrating around. (D) Adult rudiment of the middle eight-armed pluteus. Cells around the spicules (arrowhead), which are stained with calcein, have intense P4 reactivity; in contrast, the cells in tube foot and cells not related to spicules (arrows) are very weakly stained with P4 and their outlines are obscure.

arrows) and in the adult rudiment of the eight-armed pluteus (Fig. 8D: arrows); they do not stain strongly. Strong P4 antigen expression was only observed after spicule formation began (Fig. 8D: arrowheads).

Discussion

Through immunofluorescent staining of skeletogenic cells, we observed the initiation at a cellular level of skeletal morphogenesis in the late-developmental larvae of *Hemicentrotus pulcherrimus* and within the adult rudiments. The antibodies used were produced originally for primary mesenchyme cells (PMCs) that were early larval skeletogenic cells, but they were also useful for the immunohistochemistry of skeletogenic cells in later larvae and adult rudiments. All skeletogenic cells associated with each spicule at each stage were stained uniformly, and the staining intensity within each cell was similar.

By using these antibodies that stain spicules and skeletogenic cells uniformly, we could investigate cell movements occurring at the onset of spicule formation. The arrangement of the cells depended on the skeleton type being observed. Cells producing a disk of the primary tube foot adopted a ring-shaped arrangement in advance of spicule formation. In contrast, cells forming a posterodorsal rod or a dorsal arch did not form any pre-patterned arrangements, but just before spicule formation, they began to aggregate at the site where the spicules would develop. It has been reported that the extracellular matrix and the ectodermal signal control the arrangement of spicule-forming cells in the embryo (Guss and Ettensohn, 1997; Ettensohn *et al.,* 2000). It would be interesting to study whether a similar molecular mechanism plays a role in subsequent skeletogenesis.

Various adult skeletal rudiments are formed in the middle eight-armed pluteus stage. We found that rudiments of spine and a test plate had developed together in an ectodermal sack of the amniotic cavity (Fig. 6C). This ectodermal sack covered skeletogenic tissue that was stained by a PMC-specific monoclonal antibody, and each spicule grew in this tissue (Fig. 7). Although there are two types of spines and tests growing in this larval stage, each type of skeletal rudiment had a typical shape, and it is possible to recognize the type of skeleton from the shape of the rudiments. A rudiment of the ventral spine has a characteristic hexaradiate shape (Fig. 6B) and was paired with a rudiment of the interambulacral plate that has a typical triradiate form. In contrast, a rudiment of the dorsal spine (Fig. 6F) has a peculiar triradiate shape (triradiate, like a rudiment of interambulacral plate but much smaller and distinguishable from it) and always exists in pairs with a rudiment of the terminal plate, which is located on the outer side of the adult rudiment. This finding is in agreement with the observation by Gordon (1926) that ventral spines in the adult sea urchin are located on the interambulacral plates and dorsal spines on the terminal plates.

Several PMC-specific molecules, such as cell surface msp130 and spicule matrix proteins, are also expressed in adult tissues (Anstrom and Raff, 1987; Parks and Raff, 1988; Drager *et al.,* 1989; Wilt, 2002). We confirmed that the cell surface antigen is expressed throughout skeletogenesis of the late-stage larvae in the present study. Therefore, it seems that these molecules are used in the skeletal morphogenesis of the sea urchin throughout its life cycle (from embryo to larva to adult sea urchin). PMCs and the late skeletogenic cells stained in this study share several characteristics. The antigen expression of skeletogenic cells is initiated right before spicule formation. Embryonic PMCs and late larval cells resemble each other: both are rounded in shape (not deformed like secondary mesenchyme cells) and have several filopodia. In addition, most of the skeletal rudiments we observed were triradiate in form, like the ones in the embryonic stage. Thus, it is likely that the molecular

mechanism in the system associated with the morphogenesis of the skeleton continues to function throughout the life cycle of the sea urchin. It might be interesting to determine the nature of the upstream regulatory networks operating in sea urchin embryos and larvae to reveal which parts of the regulatory system related to skeletogenesis are critically common between larva and adult.

It is also still not clear whether PMCs and these late skeletogenic cells are in the same cell lineage or whether the genes and proteins associated with skeletogenesis are independently expressed in different cell lines. In the present study, we anticipated the possibility that PMC descendants might migrate to form new spicules, so we examined the initial phase of spicule formation (Fig. 8). However, we did not observe any PMC descendants maintaining strong expression of the antigen and migrating in the blastocoel to form new spicules. Only weakly stained cells were seen in the blastocoel of larvae, but P4 antigen expression was always strong in the skeletogenic cells associated with the spicules. PMCs may have down-regulated the antigen expression, migrated, and restarted it at the position where they form new spicules. The other possibility is that other type of cells are involved in skeletogenesis of the late larva or adult. In the sea urchin embryo, another type of mesenchymal cell, secondary mesenchyme cells (SMCs), potentially have an ability to become skeletogenic cells. SMCs make a lineage conversion when PMCs are removed, and these lineage-converted SMCs can be stained with a PMC-specific antibody just as PMCs can (Ettensohn and McClay, 1988). This implies that other kinds of cells might have the potential to be skeletogenic cells, but they are somehow suppressed in the embryonic stage. The cell lineage relationships among embryo, larva, and adult sea urchins have not been investigated to date because of technical difficulties, but it is important to clarify these relationships.

The presence of an early larval skeleton is one of the specific defining characteristics of echinoids. This group is thought to have evolved from early larval skeletons produced by micromere-derived PMCs from an ancestral condition, such as that found in asteroids, that did not possess these characteristics. During the evolution of the direct-developing sea urchin *Heliocidaris erythrogramma,* a part of the larval program of development has been deleted, and the adult program of development has been accelerated (Parks and Raff, 1988). The geometry of early cleavage is modified in this species such that the micromeres and the early embryonic pattern of msp130 expression is absent and an unusually large number of mesenchyme cells enter the blastocoel, where they begin directly forming the adult skeleton. A comparison of the source of adult skeletogenic cells in indirect-developing sea urchins, direct-developing urchins, and asteroids would contribute to our understanding of the evolutionary changes of the developmental process.

Acknowledgments

The authors wish to thank Dr. Hideki Katow of Tohoku University and Dr. Tetsuya Kominami of Ehime University for the kind gift of monoclonal antibodies. We also appreciate help from Dr. Shin-ichi Nemoto with kind support and from Dr. Masashi Noguchi with larval culture. We gratefully acknowledge Mr. Mamoru Yamaguchi and the staff of the Marine and Coastal Research Center, Ochanomizu University, for collecting animals. The manuscript was greatly improved by comments from Dr. Fred Wilt.

Literature Cited

Ameye, L., R. Hermann, C. Killian, F. Wilt, and P. Dubois. 1999. Ultrastructural localization of proteins involved in sea urchin biomineralization. *J. Histochem. Cytochem.* **47:** 1189–1200.

Anstrom, J. A., and R. A. Raff. 1987. Localization and expression of msp130, a primary mesenchyme lineage-specific cell surface protein of the sea urchin embryo. *Development* **101:** 255–265.

Davidson, E. H., J. P. Rast, P. Oliveri, A. Ransick, C. Calestani, C. H. Yuh, T. Minokawa, G. Amore, V. Hinman, C. Arenas-Mena, O. Otim, C. T. Brown, C. B. Livi, P. Y. Lee, R. Revilla, M. J. Schilstra, P. J. Clarke, A. G. Rust, Z. Pan, M. I. Arnone, L. Rowen, R. A. Cameron, D. R. McClay, L. Hood, and H. Bolouri. 2002. A provisional regulatory gene network for specification of endomesoderm in the sea urchin embryo. *Dev. Biol.* **246:** 162–190.

Drager, B. J., M. A. Harkey, M. Iwata, and A. Whiteley. 1989. The expression of embryonic primary mesenchyme genes of the sea urchin, *Strongylocentrotus purpuratus,* in the adult skeletogenic tissues of this and other species of echinoderms. *Dev. Biol.* **133:** 14–23.

Dubois, P. H., and C. Chen. 1989. Calcification in echinoderms. Pp. 109–178 in *Echinoderm Studies 3,* M. J. Jangoux, and J. M. Lawrence, eds. Balkema, Rotterdam.

Ettensohn, C. A., and D. R. McClay. 1988. Cell lineage conversion in the sea urchin embryo. *Dev. Biol.* **125:** 396–409.

Ettensohn, C. A., K. A. Guss, P. G. Hodor, and K. M. Malinda. 1997. The morphogenesis of the skeletal system of the sea urchin embryo. Pp. 225–265 in *Reproductive Biology of Invertebrates, Vol. 7, Progress in Developmental Biology,* J. Collier, ed. John Wiley, Chichester.

Ettensohn, C. A., K. M. Malinda, H. C. Sweet, and X. Zhu. 2000. The ontogeny of cell-guidance information in an embryonic epithelium. Pp. 31–48 in *Regulatory Process in Development,* Weener-Gren International Series, Vol. 76, L. Olsson and C. O. Jacobson, eds., Portland Press, London.

Gordon, I. 1926. The development of calcareous test of *Echinus miliaris. Philos. Trans. R. Soc. Lond.* **B214:** 259–312.

Guss, K. A., and C. A. Ettensohn. 1997. Skeletal morphogenesis in the sea urchin embryo: regulation of primary mesenchyme gene expression and skeletal rod growth by ectoderm-derived cues. *Development* **124:** 1899–1908.

Gustafson, T., and L. Wolpert. 1967. Cellular movement and contact in sea urchin morphogenesis. *Biol. Rev.* **42:** 422–498.

Hyman, L, H. 1955. *The Invertebrates: Echinodermata, the Coelomate Bilateria,* Vol. 4. McGraw-Hill, New York.

Killian, C. E., and F. H. Wilt. 1996. Characterization of the proteins comprising the integral matrix of *Strongylocentrotus purpuratus* embryonic spicules. *J. Biol. Chem.* **271:** 9150–9159.

Kominami, T., and M. Takaichi. 1998. Unequal divisions at the third

cleavage increase the number of primary mesenchyme cells in sea urchin embryos. *Dev. Growth Differ.* **40:** 545–553.

Noguchi, M. 1978. Metamorphosis of the sea urchin. Pp. 89–115 in *Biology of Metamorphosis.* Japanese Society of Developmental Biologists, eds. Iwanami-shoten, Tokyo. (In Japanese).

Okazaki, K. 1975. Normal development to metamorphosis. Pp. 177–232 in *The Sea Urchin Embryo: Biochemistry and Morphogenesis,* G. Czihak, ed. Springer-Verlag, New York.

Parks, A. L., and R. A. Raff. 1988. Molecular analysis of heterochronic changes in the evolution of direct developing sea urchins. *J. Evol. Biol.* **1:** 27–44.

Shimizu, K., and R. Matsuda. 1988. Micromere differentiation in the sea urchin embryo: expression of primary mesenchyme cell specific antigen during development. *Dev. Growth Differ.* **30:** 35–47.

Shimizu-Nishikawa, K., H. Katow, and R. Matsuda. 1990. Micromere differentiation in the sea urchin embryo: immunochemical characterization of primary mesenchyme cell-specific antigen and its biological roles. *Dev. Growth Differ.* **32:** 629–636.

Wilt, F. H. 1999. Matrix and mineral in the sea urchin larval skeleton. *J. Struct. Biol.* **126:** 216–26.

Wilt, F. H. 2002. Review, biomineralization of the spicules of sea urchin embryos. *Zool. Sci.* **19:** 253–261.